MULTIDIMENSIONAL EFFECTS IN THE THERMAL RESPONSE OF FUEL ROD SIMULATORS*

R. D. Dabbs L. J. Ott
Engineering Technology Division
Oak Ridge National Laboratory
Oak Ridge, Tennessee 37830

CONF-801091--5

ABSTRACT

One of the primary objectives of the Oak Ridge National Laboratory Pressurized-Water Reactor Blowdown Heat Transfer Separate-Effects Program is the determination of the transient surface temperature and surface heat flux of fuel pin simulators (FPSs) from internal thermocouple signals obtained during a loss-of-coolant experiment (LOCE) in the Thermal-Hydraulics Test Facility. This analysis requires the solution of the classical inverse heat conduction problem. The assumptions that allow the governing differential equation to be reduced to one dimension can introduce significant errors in the computed surface heat flux and surface temperature. The degree to which these computed variables are perturbed is addressed and quantified.

INTRODUCTION

The Oak Ridge National Laboratory (ORNL) Pressurized-Water Reactor Blowdown Heat Transfer (PWR-BDHT) Program [1] is an experimental separate-effects study of the principal phenomena that are important to loss-of-coolant accident (LOCA) analysis. Primary test results are obtained from the Thermal-Hydraulics Test Facility (THTF), a large nonnuclear experimental loop with a test section that contains an array of indirect electrically heated fuel pin simulators (FPSs) with a 365.76-cm (12-ft) heated length.

The FPSs in the first rod bundle (bundle 1) used in the THTF have a dual-sheath design (see rod cross section in Fig. 1). The outer sheath is 0.0254-cm-thick (0.010-in.) stainless steel; the inner sheath is 0.0762-cm-thick (0.030-in.) stainless steel and is grooved to accept 0.0508-cm (0.020-in.) Chromel-Alumel thermocouples. The next inner layer is boron nitride (BN), which electrically insulates the heating element from the stainless steel sheaths. The heater element consists of a series of oversleeves swaged over a central base tube to provide the heat generation zones. The core of the heater element is filled with magnesium oxide (MgO), which is both a filler and an insulator between the heating element and the central rod thermocouple sheaths.

---

* Oak Ridge National Laboratory, P.O. Box Y, Bldg. 9204-1, Oak Ridge, Tennessee 37830.

Research sponsored by Division of Reactor Safety Research, U.S. Nuclear Regulatory Commission under Interagency Agreements DOE 40-551-75 and 40-552-75 with the U.S. Department of Energy under contract W-7405-eng-26 with the Union Carbide Corporation.

DISCLAIMER

A bundle 1 prototypical heater was cross sectioned and microphotographed. A typical cross section (Fig. 2) shows the location of sheath thermocouples and heater components. Enlarged views of the inner groove area revealed that the groove had been milled to a depth of 0.0394 cm (0.0155 in.), which was less than the original 0.0508-cm (0.020-in.) OD of the thermocouple. As a result, during swaging operations, the thermocouple was crushed to a slightly elliptical shape, and the edge of the milled groove was pulled away from the outer sheath. A review of all photographs of cross sections at thermocouple bead junctions in the heater resulted in the composite drawing shown in Fig. 3.

The heater rod is reduced to its final diameter by swaging, often creating an imperfect fit between the inner and outer sheaths at the thermocouple locations and resulting in a gap between the thermocouple junction and the outer sheath.

One of the primary objectives of the ORNL PWR-BDHT Separate-Effects Program is the determination of the transient surface temperature and surface heat flux of FPSs from internal thermocouple signals obtained during a loss-of-coolant experiment (LOCE) in the THTF. This analysis requires the solution of the classical inverse heat conduction problem [2]. The state-of-the-art solution of the inverse heat conduction problem is one dimensional in scope; that is, for an FPS cylindrical geometry, the normal assumption is that azimuthal and axial heat conduction are negligible, thereby allowing the governing differential equation to be reduced to one dimension in terms of radius only. Analysis showed that these assumptions can introduce significant errors in the computed surface heat flux and surface temperature. The primary causes of these errors are the presence of the embedded thermocouple and heater element eccentricity. The degree to which these factors perturb the surface heat flux and surface temperature is addressed and quantified.

The general investigative approach involved two-dimensional modeling of BDHT FPSs using the HEATING5 computer code [3], a generalized heat conduction code developed at ORNL.

HEATING5 STUDIES

Two-Dimensional (R-θ) Studies with Heater Eccentricity = 0

The axes of symmetry for a typical "pie" segment of the cross section in Fig. 2 would be a radial line between a pair of thermocouples (0°) and a radial line halfway between two grooves. Rather than model a full 360° of the cross section, the segment shown in Fig. 3 was modeled. This allowed "finer" nodalization in the thermocouple area and kept the computer core requirements and running time to a minimum without sacrificing modeling accuracy.

The HEATING5 model needed the following physical properties for each component in the heater rod: density (ρ), thermal conductivity (k), and specific heat (Cp). All three properties were required for the transient cases; only the thermal conductivity was needed for the steady-state runs. Except for the thermal conductivities of MgO and BN, the optimum polynomial fits (to literature data) for the heat capacity and thermal conductivity of each component in terms of temperature were determined; this work is documented in both the Oak Ridge Inverse Code (ORINC) [2] and the Oak Ridge Thermocouple Calibration Code (ORTCAL) [4] manuals. The ORTCAL code performed regressions on data from steady-state and controlled transient tests to provide the BN and MgO thermal conductivities.

The internal radial dimensions of bundle 1 heaters were measured from cross sections of the prototypical BDHT FPS.

Because HEATING5 solves the forward conduction problem, it was necessary to supply the code with both the FPS surface boundary conditions (i.e., heat transfer coefficient and fluid sink temperature) and the power generation rate in the Inconel heating element. For the steady-state studies, these boundary conditions were determined from THTF steady-state calibration runs. For the transient study, local fluid conditions were taken from the predicted response of the THTF core by a thermal-hydraulic computer program.

Steady-state studies

The boundary conditions for the steady-state cases, along with the gap between the stainless steel sheaths, are given in Table 1. The results of the HEATING5 simulations are presented graphically, with the principal variables of interest (surface heat flux, surface temperature, and a ratio of the local flux to the mean flux) plotted as a function of surface arc length. For comparison, the mean surface conditions [flux, temperature, and driving potential (i.e., $T_{surface} - T_{sink}$)] for these cases are given in Table 2. These mean conditions represent averages of the surface conditions over the surface area.

Figure 4 is an overlay of the local surface heat flux for test cases 1 through 4. Figures 5 and 6 contain the corresponding local surface temperatures, and Fig. 7 is a plot of the flux ratio for all four cases. Note that the thermocouple groove in the R-θ model extends from 0.0 to 0.062 cm.

Referring to Fig. 7, in a forced-convection heat transfer mode (cases 1 through 3), the local surface heat flux is ∿7 to 11% less than the mean

flux in the vicinity of the sheath thermocouple (0.0 to 0.062 cm) and ∿4% greater than the mean flux away from the thermocouple and groove. However, if the surface of the pin is in nucleate boiling (case 4), the variation in the surface flux is greater, that is, ∿7 to 23% less than the mean around the thermocouple and ∿5 to 7% greater than the mean away from the groove.

In the forced-convection cases (1 through 3), the surface temperature variation is ∿4.8 to 6.0 K over the 32° arc of the model, which is ∿15.4% of the mean driving potential [i.e., $\Delta T_{variation}/(T_{surface} - T_{sink})$]. However, for the nucleate boiling case (4), the surface temperature variation of 1.5 K is ∿31.5% of the mean driving potential; thus, the surface flux for case 4 is more perturbed (as is evident in Figs. 4 and 7).

The primary sources of these perturbations are the air pockets formed by the groove, thermocouple, and outer sheath and the low thermal conductivity of the insulating material (MgO) in the thermocouple. The air pockets and MgO-filled thermocouple offer paths of greater resistance for heat flow (as compared with the stainless steel sheath); thus, the flux through the groove area is depressed while the flux is higher away from the groove where the thermal resistance is less.

For the inverse calculations made by ORINC (one dimensional in terms of R), two forcing functions are required — the local power generation rate and the sheath thermocouple response. Errors in the determination of the local power generation rate are primarily (1) instrument measurement errors (i.e., measurement of the rod shunt amperage and generator voltage) and (2) errors in determination of the local power peaking factor [4]. However, in addition to its measurement error, the thermocouple responds to the temperature at the bead, where the heat flux was shown to be depressed relative to the mean surface flux. Thus, a one-dimensional inverse computation of a mean flux for each time increment from the thermocouple response (and $\dot{q}'''$) would be ∿7 to 8% less than the actual mean surface flux and ∿11 to 15% less than the maximum surface flux.

As noted above, the low thermal conductivity of the MgO insulator in the sheath thermocouple is a contributing factor to the perturbation of the surface heat flux. However, if a more preferable thermocouple insulator such as BN were used, similar perturbations in the surface heat flux would be produced because of the air pockets surrounding the sheath thermocouples.

Transient study

Boundary conditions ($t \leq 0.5$ sec) for the transient study are presented in Table 3.

The surface heat flux, surface temperature, and ratio of the local flux to the mean flux of the HEATING5 transient simulation are presented in Figs. 8 through 10, respectively. Each figure is an overlay of the results at three time periods (0.2, 0.3, and 0.4 sec). The boundary conditions in Table 3 indicate that the pin is in subcooled nucleate boiling at 0.2 sec, departs from nucleate boiling at ∿0.3 sec, and is high on the temperature ramp after critical heat flux (CHF) at 0.4 sec.

Referring to Fig. 10, at 0.2 and 0.3 sec, the local heat flux is ∿9 to 23% less than the mean flux around the thermocouple and ∿5 to 7% greater

than the mean away from the groove, which is similar to the steady-state study results for the nucleate boiling mode (case 4). Also, the relative variation at 0.4 sec is approximately the same as in cases 1, 2, and 3 in the previous section (the local flux is ∿7 to 9% less than the mean in the vicinity of the thermocouple and groove).

In general, the severe perturbations noted in the steady-state studies also exist in the transient simulation and are of approximately the same relative magnitude. There is no dampening or smoothing of the surface conditions (i.e., temperature and flux) during a transient.

Two-Dimensional (R-θ) Steady-State Studies with Heater Eccentricity ≠ 0

Eccentricity, as used here, is defined as the offset between the center of the heating element and the center of the stainless steel sheaths. A line through the two centers defines a line of symmetry; therefore, only 180° of the cross section needs to be modeled. The eccentricity was not varied in these studies, and the maximum allowable eccentricity (as set forth in the construction specifications for the FPS) of 0.038 cm (0.015 in.) was used.

The boundary conditions for the steady-state eccentric studies are presented in Table 4. Overlays of simulation results for cases 6 and 7 are presented in Figs. 11 (surface heat flux), 12 (surface temperature), and 13 (flux ratio).

As shown in Fig. 13, the local heat flux varies from ∿11 to 12.5% higher than the mean flux at 0.0 (position at which the heater is in closest proximity to the sheath) to ∿10.5 to 12.0% lower than the mean flux at θ = 165° (arc = 0.62 in.).

The local heat transfer mode in case 6 is subcooled forced convection, and the azimuthal surface temperature variation (Fig. 12) is ∿7.8 K (14°F). For case 7, which is in subcooled nucleate boiling, the variation in the surface temperature is only ∿1.2 K (2.2°F). Given the standard deviation of a bundle 1 temperature measurement of 2.4 K (4.3°F) and the FPS surface in the nucleate boiling regime, determining if the heating element is eccentric in relation to the sheaths is not possible. For proof of eccentricity (just from thermometry measurements), having multiple thermocouples per level per rod (preferably three, spaced at 120°) will be necessary, and, during steady-state testing, the rods will have to be maintained in the forced-convection heat transfer regime.

CONCLUSIONS

In FPSs of THTF bundle 1 design in which the heating element is perfectly centered (i.e., eccentricity = 0), the steady-state surface heat flux and surface driving potential are severely perturbed azimuthally. The degree of the perturbation is partially dependent on the heat transfer mechanism at the surface. However, the primary sources of the perturbations are (1) the air pockets formed by the groove, thermocouple, and outer sheath and (2) the low thermal conductivity of the insulating material (MgO) in the thermocouples.

The impact of this azimuthal perturbation in the heat flux is in the analysis of the sheath thermocouple response. The thermocouple responds to the temperature at the bead, and the heat flow through the

bead is depressed relative to the mean surface flux. Thus, a one-dimensional inverse computation of a "mean flux" for each time increment from the thermocouple response (and $\dot{q}'''$) would be ∿7 to 8% less than the mean surface flux and ∿11 to 15% less than the maximum. If BN had been used as thermocouple insulation, the flux through the thermocouple would have been improved — only 1 to 2% less than the mean surface flux.

These severe perturbations are evident in both steady-state and transient simulations and are of approximately the same relative magnitude. There is no dampening or smoothing of the perturbations of the surface conditions (i.e., temperature and flux) during a transient.

If the additional problem of heater element eccentricity is considered, the surface flux variation can be as much as ±12% of the mean flux. Furthermore, if the heater surface is in the subcooled nucleate boiling heat transfer regime, the variation in the surface temperature is less than the standard deviation of a bundle 1 temperature measurement (standard deviation of a bundle 1 thermocouple is 2.4 K). Determining whether the heating element is eccentric in relation to the sheaths is not possible if the heater is in the nucleate boiling regime. To establish proof of eccentricity (just from thermometry measurements), having multiple thermocouples per level per rod will be necessary (preferably three, spaced at 120°), and the rod surface must be maintained in the forced-convection heat transfer regime.

REFERENCES

1. *Project Description, ORNL-PWR Blowdown Heat Transfer Separate-Effects Program — Thermal Hydraulic Test Facility (THTF),* ORNL/NUREG/TM-2 (February 1976).

2. Ott, L. J., and Hedrick, R. A., *ORINC — A One-Dimensional Implicit Approach to the Inverse Heat Conduction Problem,* ORNL/NUREG-23 (November 1977).

3. Turner, W. D., Elrod, D. C., and Siman-Tov, I. I., *HEATING5 — An IBM 360 Heat Conduction Program,* ORNL/CSD/TM-15 (March 1977).

4. Ott, L. J., and Hedrick, R. A., *ORTCAL — A Code for THTF Heater Rod Thermocouple Calibration,* NUREG/CR-0342 (ORNL/NUREG-51) (February 1979).

BIOSKETCH

The authors are development engineers in the Analysis group of the Oak Ridge National Laboratory (ORNL) Pressurized-Water Reactor Blowdown Heat Transfer (PWR-BDHT) Separate-Effects Program.

Mr. Dalos is a 1977 Nuclear engineering graduate of the University of Tennessee at Knoxville.

Mr. Ott is also a graduate of the University of Tennessee at Knoxville (1968, B.S. Chemical Engineering; 1978, M.S. Chemical Engineering).

Table 1. Case information and boundary conditions for steady-state R-θ runs (ε = 0) for bundle 1 FPS simulations

Test case No.	Nominal rod power (kW)	Local volume power generation rate [W/cm^3 (Btu/hr-in.^{3})]	Gap [cm (mils)]	Local sink temperature [K (°F)]	Local heat transfer coefficient [W/m^2-K (Btu/hr-°F-ft^2)]	Local heat transfer mode
1	81.9	6.079×10^3 (3.40×10^5)	1.041×10^{-4} (0.041)	577.1 (579.2)	3.5159×10^4 (6,193)	Forced convection
2	91.6	6.79×10^3 (3.80×10^5)	1.016×10^{-4} (0.040)	501.1 (442.3)	3.7467×10^4 (6,600)	Forced convection
3	102.3	7.581×10^3 (4.24×10^5)	9.398×10^{-5} (0.037)	580.9 (585.9)	3.5527×10^4 (6,258)	Forced convection
4	124.6	9.244×10^3 (5.17×10^5)	9.652×10^{-5} (0.038)	619.3 (655.1)	3.5431×10^5 (62,412)	Subcooled nucleate boiling

Table 2. Average surface conditions for steady-state R-θ runs (ε = 0) for bundle 1 FPS simulations

Test case No.	Mean surface flux [W/m^2 (Btu/hr-ft^2)]	Mean surface temperature [K (°F)]	Mean driving potential [K (°F)]
1	1.109×10^6 (3.518×10^5)	608.70 (636.00)	31.56 (56.80)
2	1.24×10^6 (3.932×10^5)	534.19 (501.87)	33.09 (59.57)
3	1.384×10^6 (4.387×10^5)	619.82 (656.00)	38.94 (70.10)
4	1.687×10^6 (5.349×10^5)	624.08 (663.67)	4.76 (8.57)

Table 3. Boundary conditions for transient R-θ run
(ε = 0 and gap = 1.4×10^{-4} cm)

Time (sec)	Local volume power generation rate [W/cm^3 (Btu/hr-in.^{3})]	Local heat transfer coefficient [W/m^2-K (Btu/hr-°F-ft^2)]	Local sink temperature [K (°F)]
0.0	9.222×10^3 (5.1577×10^5)	3.651×10^5 (64,313.2)	621.0 (658.2)
0.050	9.2174×10^3 (5.1552×10^5)	4.903×10^4 (8,637.5)	605.2 (629.7)
0.100	9.23×10^3 (5.1622×10^5)	2.744×10^5 (48,336.3)	605.2 (629.7)
0.150	9.223×10^3 (5.1584×10^5)	2.664×10^5 (46,930.9)	604.8 (628.9)
0.200	9.223×10^3 (5.1584×10^5)	2.678×10^5 (47,180.7)	605.3 (629.8)
0.250	9.23×10^3 (5.1622×10^5)	2.729×10^5 (48,066.2)	605.8 (630.8)
0.300	9.2174×10^3 (5.1552×10^5)	7.181×10^4 (12,650.3)	604.7 (628.8)
0.350	9.23×10^3 (5.1622×10^5)	1.679×10^4 (2,957.2)	604.5 (628.4)
0.400	9.223×10^3 (5.1584×10^5)	6.513×10^3 (1,147.2)	604.1 (627.7)
0.450	9.223×10^3 (5.1584×10^5)	7.489×10^3 (1,319.2)	603.8 (627.2)
0.500	9.223×10^3 (5.1584×10^5)	7.871×10^3 (1,386.5)	603.7 (627.0)

Table 4. Case information and boundary conditions for eccentric R-θ studies

Test case No.	Nominal rod power (kW)	Local volume power generation rate [W/cm^3 (Btu/hr-in.^{3})]	Gap [cm (mils)]	Local sink temperature [K (°F)]	Local heat transfer coefficient [W/m^2-K (Btu/hr-°F-ft^2)]	Local heat transfer mode	Eccentricity [cm (in.)]
6	102.3	7.58×10^3 (4.24×10^5)	9.652×10^{-5} (0.038)	580.9 (585.9)	3.5527×10^4 (6,258)	Forced convection	0.038 (0.015)
7	124.6	9.244×10^3 (5.17×10^5)	9.652×10^{-5} (0.038)	619.3 (655.1)	3.5431×10^5 (62,413)	Subcooled nucleate boiling	0.038 (0.015)

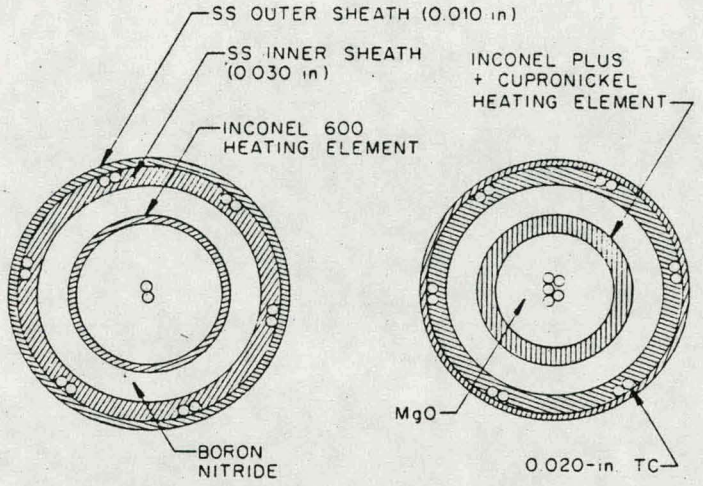

FIG. 1. HEATER ROD CROSS SECTION (1 in. = 2.54 cm).

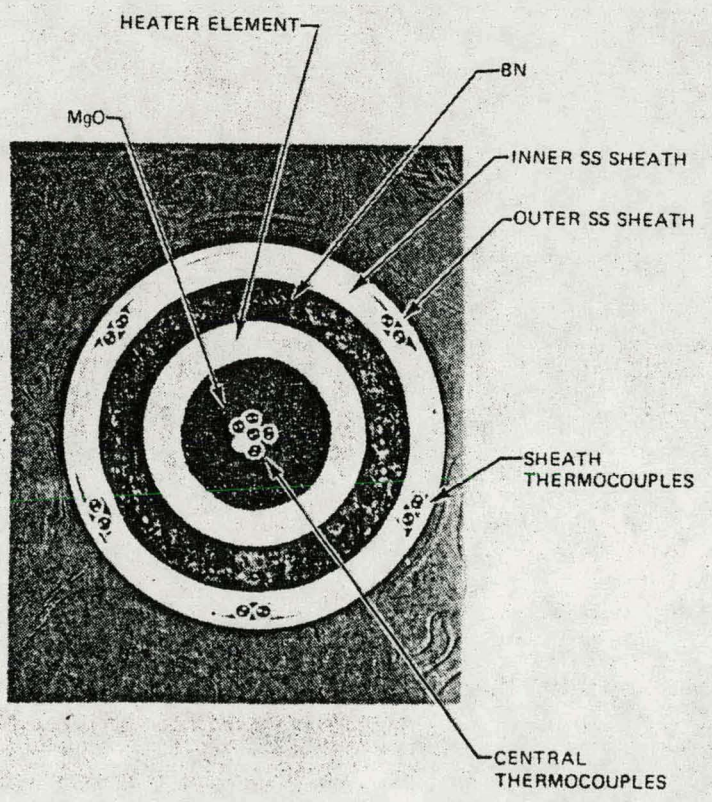

FIG. 2. CROSS SECTION OF BDHT HEATER 150-5.

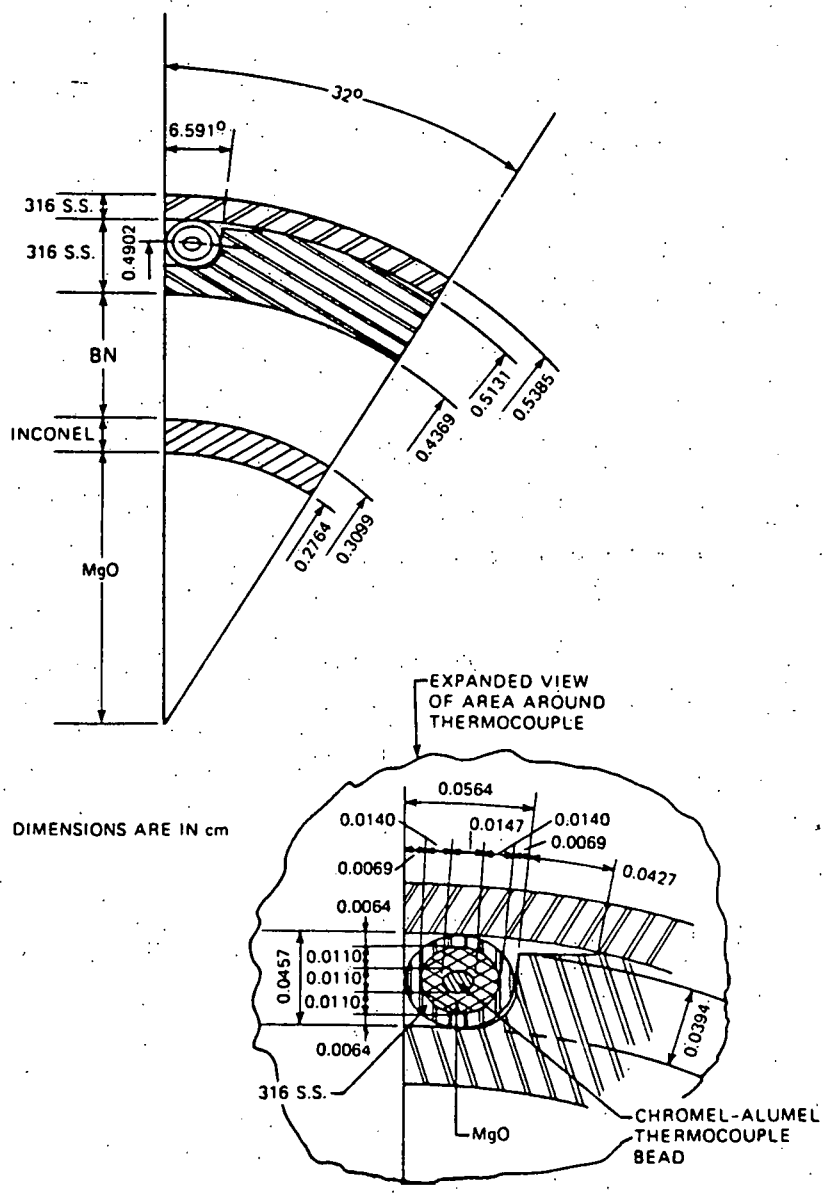

FIG. 3. SEGMENT OF HEATER ROD SHOWING MEAN DIMENSIONS IN THE THERMOCOUPLE AREA.

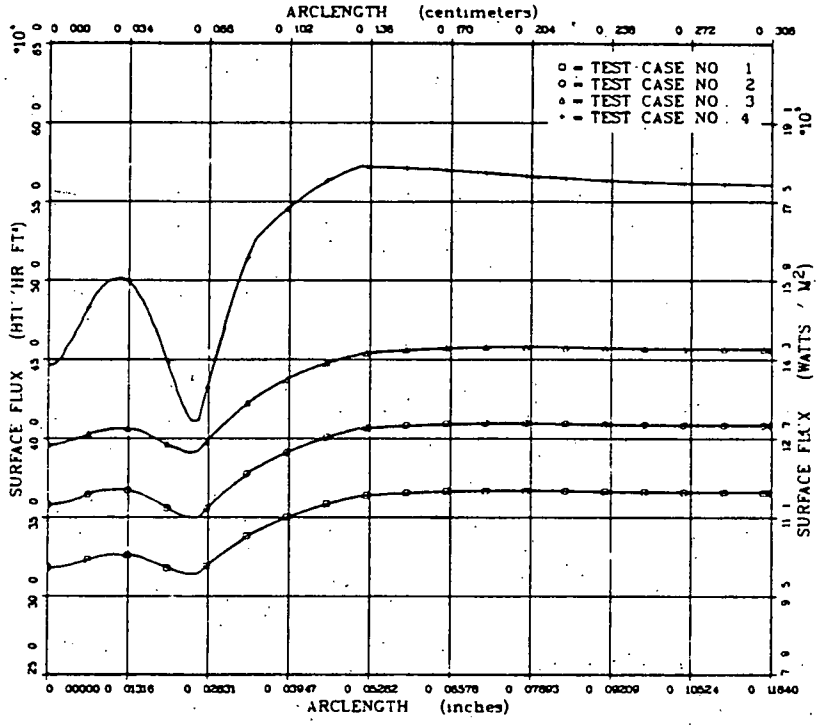

FIG. 4. R-θ MODEL — SURFACE HEAT FLUX PERTURBATION (CASES 1 THROUGH 4).

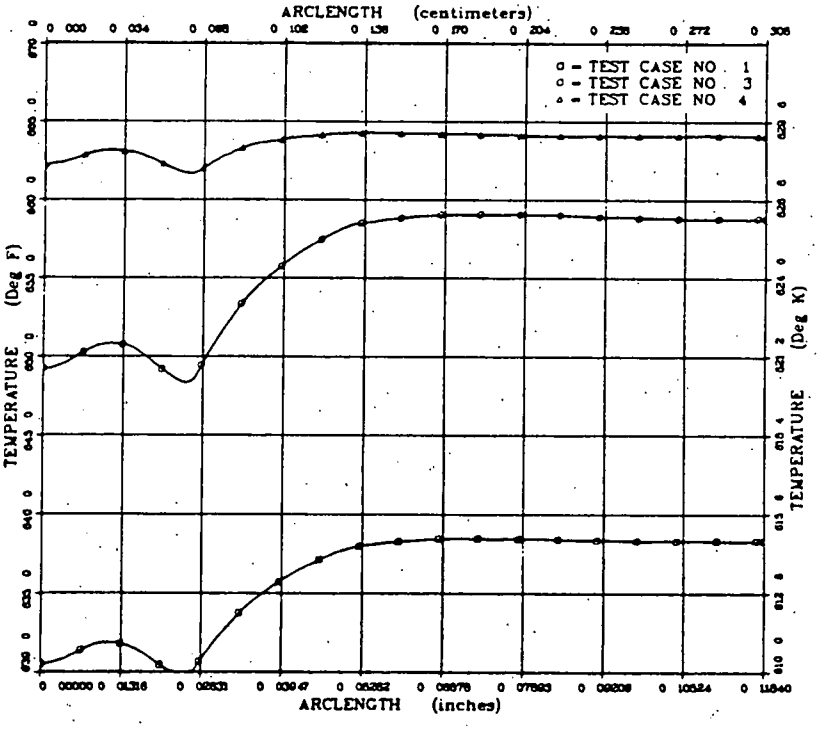

FIG. 5. R-θ MODEL — SURFACE TEMPERATURE (CASES 1, 3, AND 4).

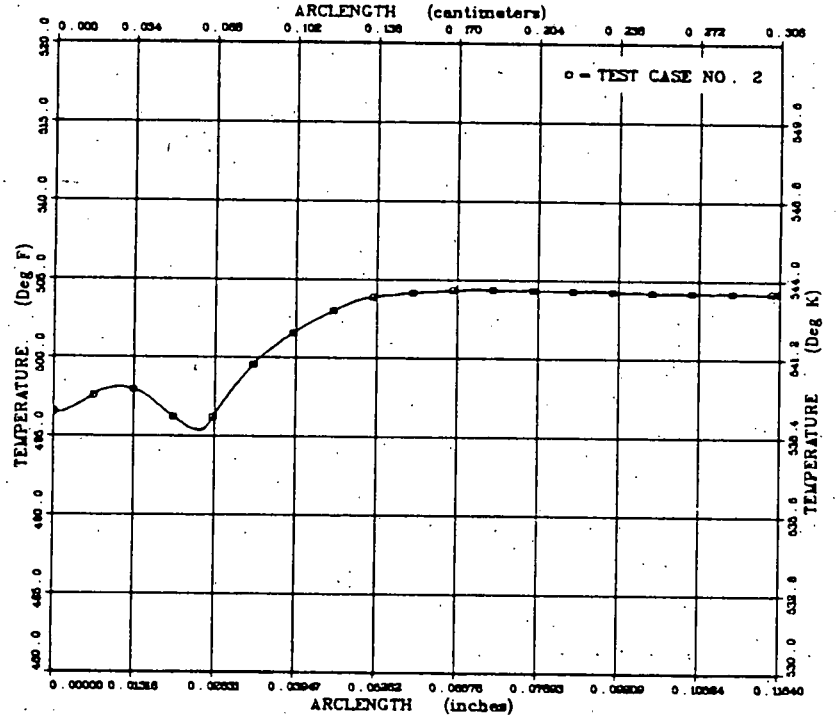

FIG. 6. R-θ MODEL — SURFACE TEMPERATURE (CASE 2).

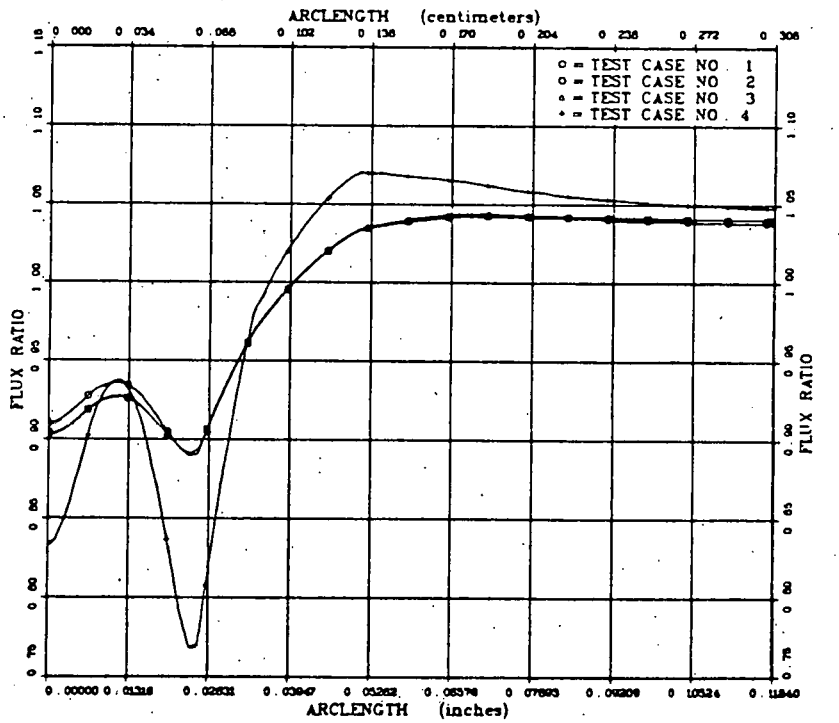

FIG. 7. R-θ MODEL — RATIO OF SURFACE FLUX TO MEAN SURFACE FLUX (CASES 1 THROUGH 4).

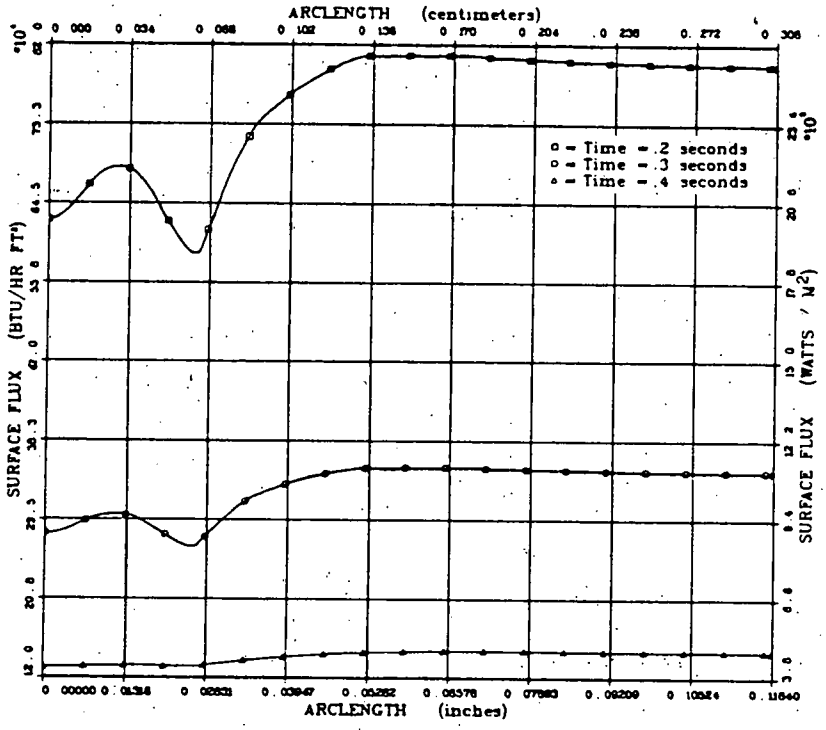

FIG. 8. R-θ MODEL — SURFACE HEAT FLUX PERTURBATION (CASE 9).

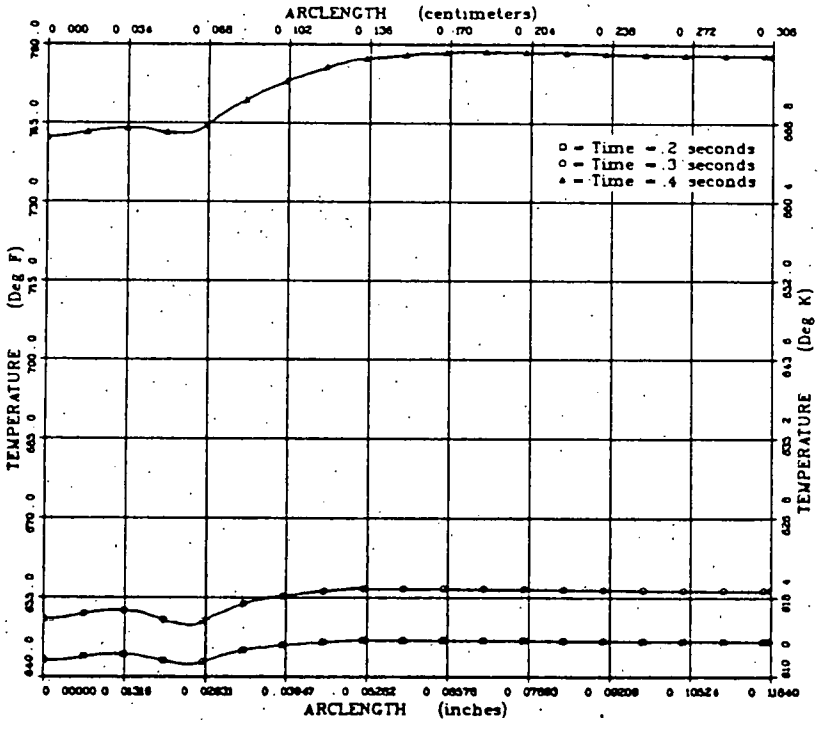

Fig. 9. R-θ MODEL — SURFACE TEMPERATURE (CASE 9).

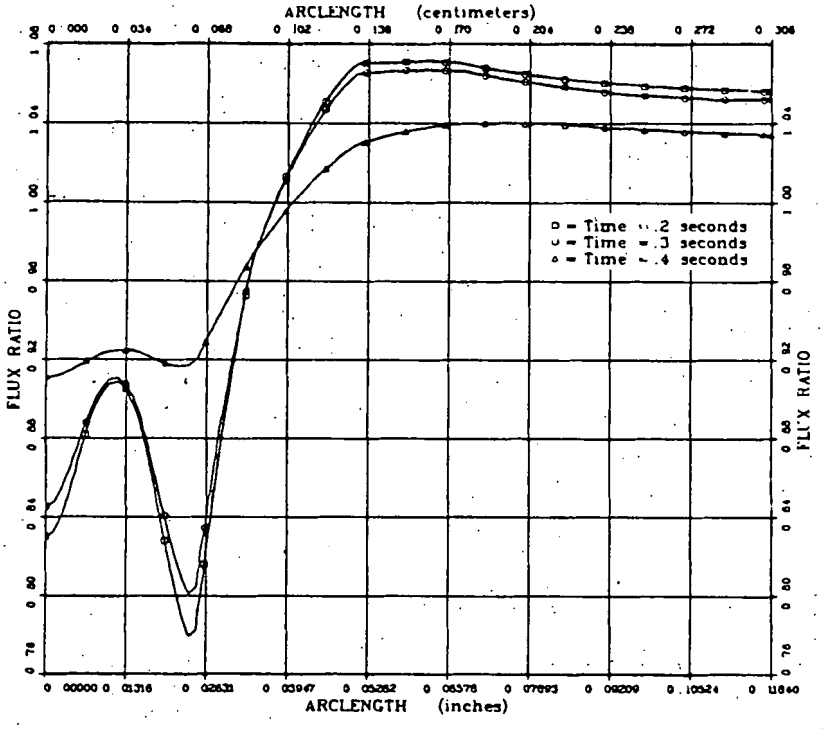

FIG. 10. R-θ MODEL — RATIO OF SURFACE FLUX TO MEAN SURFACE FLUX (CASE 9).

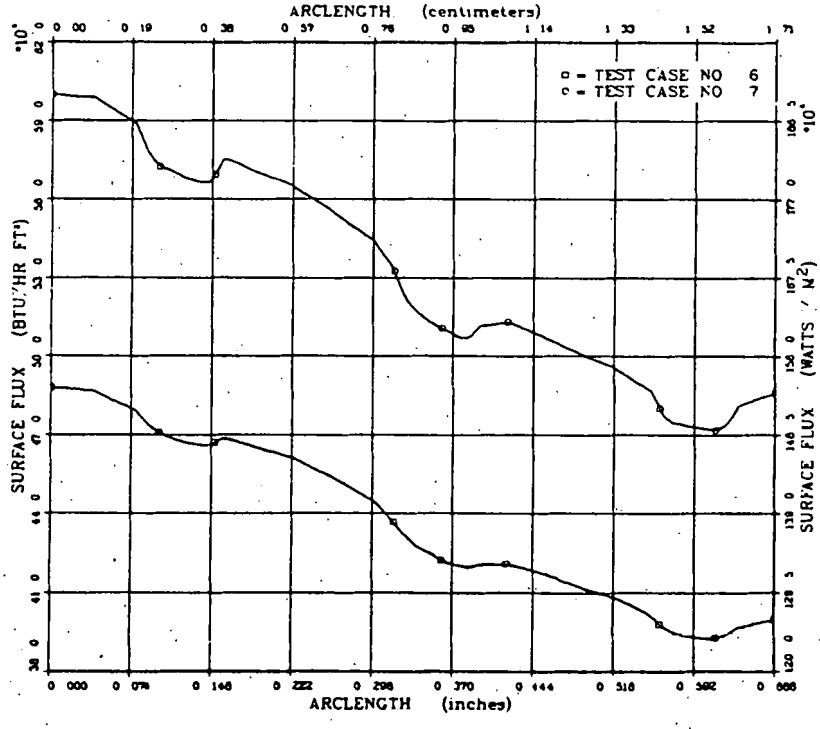

FIG. 11. R-θ MODEL — SURFACE HEAT FLUX PERTURBATION (CASES 6 AND 7).

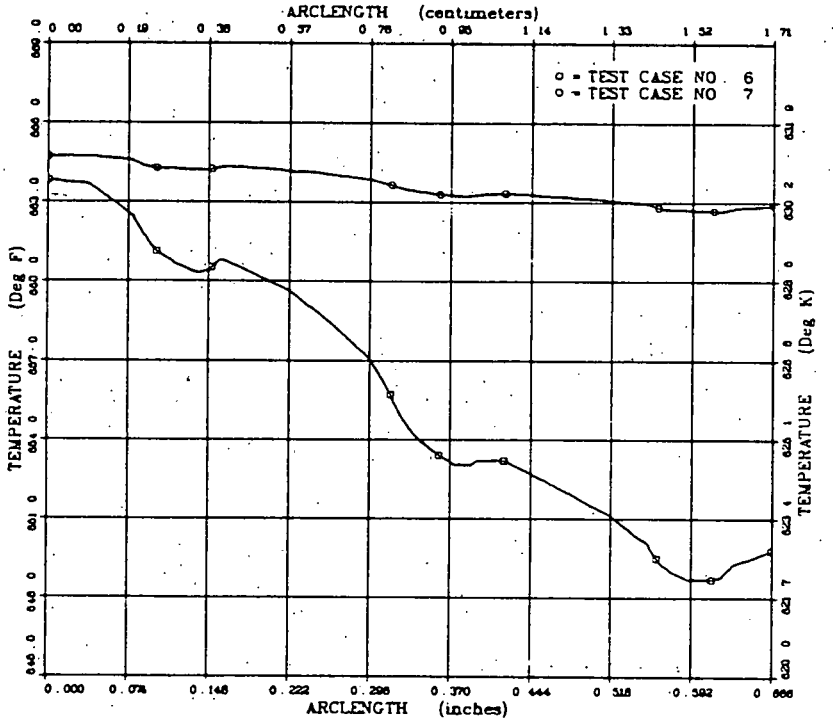

FIG. 12. R-θ MODEL — SURFACE TEMPERATURE (CASES 6 AND 7).

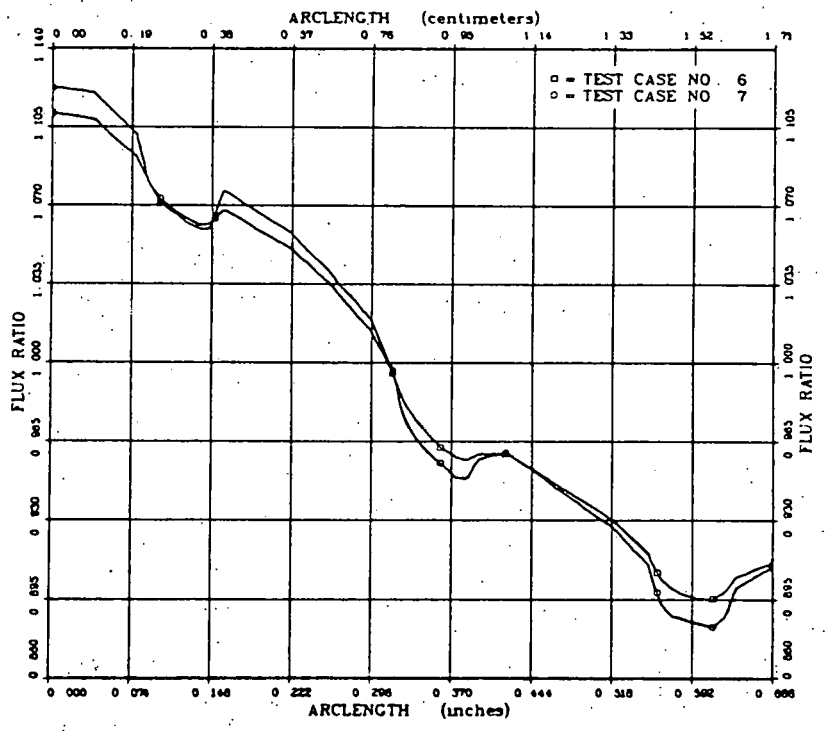

FIG. 13. R-θ MODEL — RATIO OF SURFACE FLUX TO MEAN SURFACE FLUX (CASES 6 AND 7).